High-Frequency Coherent Edge Fluctuations in a High-Pedestal-Pressure Quiescent H-Mode Plasma

Z. Yan, G. R. McKee, R. J. Groebner, P. B. Snyder, T. H. Osborne, and K. H. Burrell

Phys. Rev. Lett. **107**, 055004 — Published 29 July 2011

DOI: 10.1103/PhysRevLett.107.055004

High frequency coherent edge fluctuations in a high pedestal pressure Quiescent H-mode plasma

Z. Yan,[1] G.R. McKee,[1] R.J. Groebner,[2] P.B. Snyder,[2] T. Osborne,[2] and K.H. Burrell[2]

[1]*University of Wisconsin-Madison, Wisconsin USA*

[2]*General Atomics, P.O. Box 85608, San Diego, California 92186-5608 USA*

(Received by

Abstract. A set of high frequency coherent (HFC) modes (f = 80–250 kHz) is observed with beam emission spectroscopy measurements of density fluctuations in the pedestal of a strongly shaped quiescent H-mode plasma on DIII-D, with characteristics predicted for kinetic ballooning modes (KBM): propagation in the ion diamagnetic drift direction; a frequency near 0.2–0.3 times the ion diamagnetic frequency; inferred toroidal mode numbers of $n \sim 10$–25; poloidal wavenumbers of $k_\theta \sim 0.17$–0.4 cm^{-1}; and high measured decorrelation rates ($\tau_c^{-1} \sim \omega_s \sim 0.5\times10^6$ s^{-1}). Their appearance correlates with saturation of the pedestal pressure.

PACS: 52.35.-g, 52.25.Gj, 52.55.Tn, 52.25.Fi, 52.55.Fa

Pressure gradients and associated instabilities arise naturally in many fluid and plasma systems to which external energy and particle fueling sources are applied. Examples abound in planetary atmospheres, astrophysical plasmas, as well as magnetized laboratory plasmas [1]. Pressure gradients (and in the case of plasmas, current density gradients) provide a free energy source that can drive a wide variety of instabilities, the nature of which depends on details of the geometry, (magneto)hydrodynamic, and microscopic stability properties of the system. The edge region of magnetically confined toroidal fusion-grade plasmas will often spontaneously develop a so-called pedestal, characterized by high temperature and density gradients, when sufficient power flux is applied [2]. This high-gradient pedestal is a localized region of reduced particle and energy flow and thus higher confinement ('H-mode'). The peak pedestal pressure is strongly correlated with the global energy confinement of the plasma, hence the fusion reaction efficiency, and is thus of great significance for optimizing the performance of burning plasmas [3,4]. Understanding the nature and impact of instabilities that govern and limit the pedestal structure, and obtaining an accurate predictive model for the pedestal height and width, is thus of great scientific and practical interest to the development of fusion energy.

The pedestal pressure gradient, hence the pedestal width, is predicted to be constrained by the onset of strong electromagnetic shear Alfven instabilities, such as kinetic ballooning mode (KBM) turbulence [5,6]. However, there are few experimental studies that comprehensively examine the structure of fluctuations and instability characteristics in the pedestal of a high-performance H-mode discharge, in particular the physical model of KBMs limiting the pedestal pressure gradient.

Based on linear theory, KBMs are expected to have several well-defined physical characteristics that guide experimental investigation: they are long-wavelength modes ($k_\perp \rho_I < 1$), and thus have radial and poloidal scales on the order of several cm for typical DIII-D pedestal condition; they should propagate in the ion diamagnetic direction in the plasma frame; exhibit a ballooning like structure; and have intermediate toroidal mode numbers, n~10-30. They are driven unstable as the local pressure gradient exceeds a critical value, and have linear growth rates that reach and exceed the large local $E \times B$ shearing rates, which are thought to stabilize most long-wavelength electrostatic drift-wave type turbulence in the H-mode pedestal [e.g., ion temperature gradient driven mode (ITG)]. The nonlinear decorrelation rates are correspondingly expected to be very fast.

This Letter reports the first observations of a set of high frequency coherent (HFC) modes localized to the pedestal region of a strongly shaped and high density Quiescent H-mode (QH-mode) plasma [7]. This unique plasma discharge configuration develops a quasi-stationary pedestal condition that allows for very comprehensive study of the characteristics and behavior of pedestal instabilities. These recently observed HFC modes described here are also quasi-steady state, and exhibit several features similar to the theoretically predicted for KBMs described above. These modes are localized to the pedestal region, and the amplitudes of such modes peak just inside the separatrix. They appear as the pedestal pressure and density are increased (yielding a relatively higher collisionality), and they act to saturate the pedestal pressure. High collisionality regimes are where KBMs are predicted to dominate: KBMs become increasingly unstable at higher pressure gradients.

This experiment on DIII-D explored the behavior of edge fluctuations in these high pedestal pressure, highly shaped (high triangularity) plasmas [8]. The discharge starts as a low density, counter-current neutral beam injected QH-mode in a high triangularity double null discharge. Once a quasi-steady QH plasma was developed, the pedestal density was increased by moving the X-point position away from divertor cryopumps to reach a theoretically predicted [9] high performance regime. These discharges had a toroidal field of B_t = 2T and a toroidal plasma current of I_p = 1.2 MA, with neutral beams injected tangentially in the opposite direction to the plasma current. Electron density and temperature are measured with Thomson Scattering (TS) [10], and a charge exchange recombination (CER) [11] system is used to measure the ion temperature, density, and rotation of fully ionized carbon, as well as the radial electric field from the carbon ion radial force balance calculation. Since carbon is the dominant low-Z impurity, the main ion density is obtained from measurements of the electron and carbon densities.

Long-wavelength, localized density fluctuations ($k_\perp \rho_i < 1$) are measured with Beam Emission Spectroscopy (BES), which measures Doppler shifted collisionally excited neutral beam D_α emission. The light intensity is related to the local density fluctuations through the atomic physics of beam atom excitation [12,13]. A 5×6 2D array of BES channels, each channel imaging a 0.9 cm (radial) × 1.2 cm (poloidal) area is located at the pedestal ($0.9 < \psi < 1.02$) [14]. Another 32 channel radial array of BES channels is deployed from $0.3 < \psi < 0.9$ (ψ the normalized poloidal flux). Figure 1(a) is a time and frequency resolved density fluctuation spectrogram from BES measurements at $\psi \sim 0.95$. It shows that the Edge Harmonic Oscillation (EHO) at ~15 kHz, which is typically

observed in QH-mode discharges [15], dominates the fluctuation spectrum before 2900 ms [Fig. 1(a)] and exhibits a few harmonics. The EHO is thought to be a saturated kink/peeling mode [16]. Figure 1(b) shows the pedestal electron pressure.

As the pedestal pressure is increased by increasing pedestal density [Fig. 1(b)], the EHO disappears, and a set of high frequency coherent modes develops with a peak amplitude near 150 kHz and a uniform frequency separation of $\Delta f \sim 8$ kHz in the range of 80–250 kHz during the 3000–4000 ms time window [Fig. 1(a)]. These HFC modes exhibit a distinctly different spectrum from the EHO, which has a dominant low toroidal mode number ($n \sim 1$–3) with several harmonics [17]. It is also observed from Fig. 1(b) that after ~3000 ms, the pedestal pressure stops increasing when the HFC modes appear, suggesting that they saturate the pedestal electron pressure. There are a few discrete ELM events shown by the vertical spikes on Fig. 1(a) during this time window, and it is seen that these ELM-like events temporarily reduce the HFC mode amplitude and pedestal pressure. Between these events, HFC modes grow up rapidly with the increasing pedestal pressure. That the individual modes persist on very long time scale (~1 s) and are closely spaced spectrally, yet are well resolved and highly coherent, suggests that the underlying instability is not strongly driven into a fully saturated state, which would be characterized by a broadband fluctuation spectrum. These modes were observed in numerous discharges during this experiment, but are not typically observed in QH-modes, likely due to the lower collisionality of most QH-mode plasmas.

The HFC modes are observed in the edge region $0.9 < \psi < 1$ only, peaking just inside the separatrix. The radial profile of the normalized density fluctuation amplitude of these HFC modes is shown in Fig. 2; importantly, they are not observed on the 32 channel BES

radial array covering the plasma interior from $0.3<\psi<0.9$. These modes are also not observed on the reflectometer (DBS2) or the CECE diagnostics, perhaps due to their localized nature, small amplitude and high frequency.

The pedestal shape parameters are obtained from hyperbolic tangent function fits to the edge pedestal profiles [18]. Figure 3 shows the pedestal electron density, temperature, and pressure profiles for three different times: early in the EHO-dominant time (~2400 ms), early high pressure time (~2800 ms) and the time during the saturated state with the HFC modes dominant (~3210 ms). The pedestal electron pressure is observed to increase [Fig. 3(c)] with the pedestal electron density [Fig. 3(a)] during the time when the HFC modes appear. The pedestal electron temperature does not change significantly [Fig. 3(b)]. Unlike electron temperature, the ion temperature is reduced during this process, potentially due to the increased electron-ion collisional energy exchange.

The frequency and spatial characteristics are used to infer the toroidal mode structure of the HFC modes. The cross spectrum between two poloidally separated BES channels from 3200–3220 ms, shown in Fig. 4, is averaged over several poloidal pairs of the 2D BES array at the radial location of $\psi \sim 0.95$. In the frequency range of 80 and 220 kHz, the high frequency coherent modes exhibit a uniform frequency separation of ~8 kHz. The HFC modes are not observed on the magnetic probe measurements. This may result from low-sensitivity of the probes to the short poloidal wavelength of these higher-frequency modes (there is no local magnetic measurement for the pedestal on DIII-D). Therefore it is not known whether these HFC modes have a magnetic component. The cross phase between two poloidal BES channels (ΔZ=1.2 cm) is shown in Fig. 4 by the red solid line and fit with the red dashed line between 60 and 250 kHz. The cross phase is

a linear function of the mode frequency. From these phase differences, the poloidal wave number k_θ is estimated to be 0.17 cm^{-1} (λ≈37 cm) at 80 kHz and 0.43 cm^{-1} (λ≈15 cm) at 160 kHz at the position $\psi \sim 0.95$ along the outbound mid-plane. ELITE calculates the KBM spatial structure for given pedestal conditions [6], including the toroidal and poloidal mode numbers. Matching the measured poloidal wavenumber at the outboard midplane with a range of modes calculated by ELITE, the inferred toroidal mode numbers for these HFC modes are estimated to be n=10 and n=19, respectively, at 80 and 160 kHz. The safety factor, q_{95}, is about 5.5, corresponding to associated poloidal mode numbers in the range m~55–104.

The turbulence group velocity estimated from BES time-delay cross correlation is shown in Fig. 5 by the diamond symbol and is compared with the local $E\times B$ velocity measured with CER system. It shows the absolute value of the mode velocity is measurably less than the $E\times B$ velocity inside the separatrix. The $E\times B$ velocity is in the electron diamagnetic direction based on the magnetic field direction and the profiles at the edge. Hence the observed HFC modes are propagating in the ion-diamagnetic direction in the plasma frame.

The decorrelation time for the envelope of the HFC modes from 80 to 250 kHz, τ_c, is determined from multiple poloidal measurements. It is defined as the e-folding time of the decay in peak amplitude of the time-delay cross correlation function between the poloidally displaced BES channels [14]. In Fig. 6 the corresponding measured nonlinear decorrelation rate, τ_c^{-1}, is compared with the local $E\times B$ shearing rate, which is inferred from the force-balance equation of the carbon ion distribution measurements obtained with CER [19,20]. The nonlinear decorrelation rate amplitude of the HFC modes is

comparable to or exceeds the local $E\times B$ shearing rate across the pedestal region. It is particularly fascinating that the modes exhibit the same frequency spectrum across the pedestal, yet the relative intensities of the various harmonics self-adjust in such a way that the decorrelation rate, a function of the full spectrum, matches the local shearing rate.

Linear stability theory predicts that as the pressure gradient exceeds a critical value, the linear growth rate of KBM increases rapidly and eventually becomes larger than the $E\times B$ shearing rate. This is unlike other long-wavelength modes, such as ITG and trapped electron modes (TEM), whose linear growth rates are expected to decrease with pressure gradient due to alpha-stabilization effects, and are typically well below the $E\times B$ shearing rate in the pedestal region [21]. Therefore, they should be quenched by $E\times B$ shear. In this experiment we have observed that the HFC modes appear when the pedestal pressure is increased, consistent with the expected onset behavior of the KBM. We also note that it is unlikely that the HFCs belong to a known class of energetic particle-driven modes, as they are pedestal localized.

ELITE calculations [6], based on intermediate n peeling-ballooning mode MHD stability of the tokamak edge region, have been performed and show the discharge is not close to an ideal ballooning stability boundary. The strong plasma shaping and high-pressure gradient may put the ideal ballooning mode very deeply in the second stable regime, as was the design of the experiment.

In conclusion, this Letter reports the first experimental observations of HFC modes observed in a high-density QH-mode plasma. All of the measured spatiotemporal characteristics of these HFC modes qualitatively match the predicted characteristics for KBMs, and in fact are observed in a high pressure, high density pedestal regime,

specifically where KBMs are expected to be most strongly driven. Future nonlinear simulations will be performed for these plasma conditions to more completely and definitively identify the nature of these modes and their role in limiting pedestal structure and stability. Further experiments are also being planned to examine the parametric scaling behavior of these modes and compare with expected scaling features of KBMs, and will be reported in the future.

ACKNOWLEDGMENT

The authors appreciate the support of the DIII-D team. This work supported by the U.S. Department of Energy under DE-FG02-89ER53296, DE-FG02-08ER54999, DE-FC02-04ER54698 and DE-FG02-95ER54309.

Figure Captions

FIG. 1. (Color On-line ONLY) (a) Cross spectrum from BES measurements as a function of time at ψ~0.95; (b) Evolution of pedestal electron pressure height.

FIG. 2. Radial profile of the relative density fluctuation amplitude of HFC modes.

FIG. 3. (Color On-Line ONLY) (a) Profiles of electron density, (b) electron temperature, and (c) electron pressure in ψ coordinates for three different times: early EHO dominant (~2400 ms), early high pressure (~2800 ms) and late HFC dominant (~3210 ms).

FIG. 4. (Color On-Line ONLY) Poloidal cross spectrum (black) and cross phase (red/gray) of density fluctuations from BES measurements (ΔZ=2.4 cm) at the time when HFC is dominant near ψ~0.95; The red/gray dashed line is a linear fit of the cross phase between 60 and 250 kHz.

FIG. 5. $E\times B$ velocity (solid line) and laboratory frame turbulence group velocity of HFC (diamond symbols) from time-delay cross correlation in ψ coordinate. The error bar estimated from profiles fitting and sensitivity studies is shown at a few locations for illustration.

FIG. 6. $E\times B$ shearing rate (solid line) and HFC decorrelation rate from BES measurements (diamond symbols) in ψ coordinate. The error bar estimated from profiles fitting and sensitivity studies is shown at a few locations for illustration.

References

[1] W. Fundamenski, *et al.*, Plasma Phys. Control. Fusion **49**, R43 (2007).

[2] F. Wagner, *et al.*, Phys. Rev. Lett. **53**, 1453 (1984).

[3] J. E. Kinsey, *et al.*, Nucl. Fusion **43**, 1845 (2003).

[4] T. H. Osborne, *et al.*, Plasma Phys. Control. Fusion **40**, 845 (1998).

[5] P. B. Snyder, *et al*., Phys. Plasmas **9**, 2037 (2002).

[6] P. B. Snyder, *et al.*, Plasma Phys. Control. Fusion **46**, A131 (2004).

[7] C. M. Greenfield, *et al.*, Phys. Rev. Lett. **86**, 4544 (2001).

[8] K. H. Burrell, *et al.*, Nucl. Fusion **49**, 085024 (2009).

[9] P. B. Snyder, *et al.*, Nucl. Fusion **47**, 961 (2007).

[10] C. L. Hsieh, *et al.*, Rev. Sci. Instrum. **75**, 3897 (2004).

[11] W. M. Solomon, *et al.*, Rev. Sci. Instrum. **79**, 10F531 (2008).

[12] R. J. Fonck, *et al.*, Rev. Sci. Instrum. **61**, 3487 (1990).

[13] T. A. Gianakon, *et al.*, Rev. Sci. Instrum. **63**, 4931 (1992).

[14] G. R. McKee, *et al.*, Plasma and Fusion Research: Regular Articles **2**, S1025 (2007).

[15] K. H. Burrell, *et al.*, Phys. Plasmas **8**, 2153 (2001).

[16] P. B. Snyder, *et al.*, Nucl. Fusion **47**, 961 (2007).

[17] K. H. Burrell, *et al.*, Plasma Phys. Control. Fusion **44**, A253 (2002).

[18] R. J. Groebner, *et al.*, Phys. Plasmas **5**, 1800 (1998).

[19] K. H. Burrell, Phys. Plasmas **4**, 1499 (1997).

[20] K. H. Burrell, *et al.*, Rev. Sci. Instrum. **75**, 3455 (2004).

[21] R. J. Groebner, *et al.*, Phys. Rev. Lett. **64**, 3015, (1990).

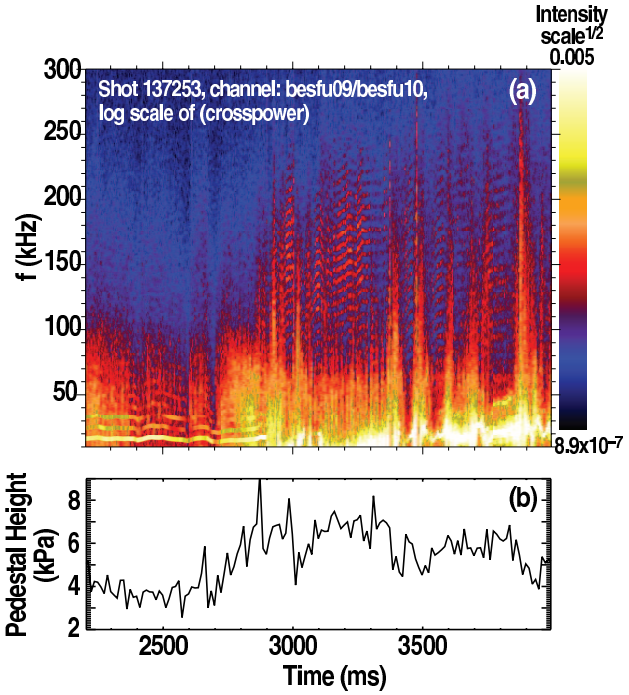

Figure 1 LX12737 28JUN2011

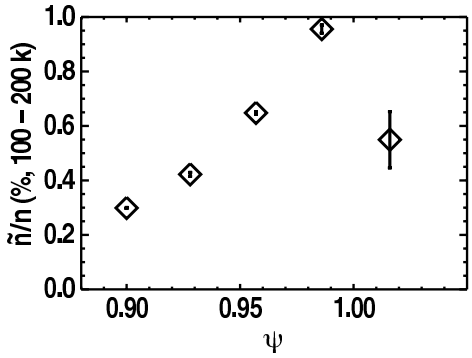

Figure 2 LX12737 28JUN2011

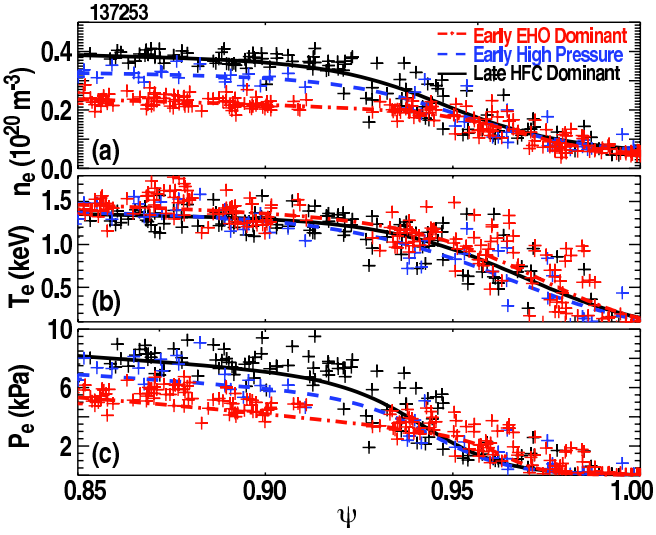

Figure 3 LX12737 28JUN2011

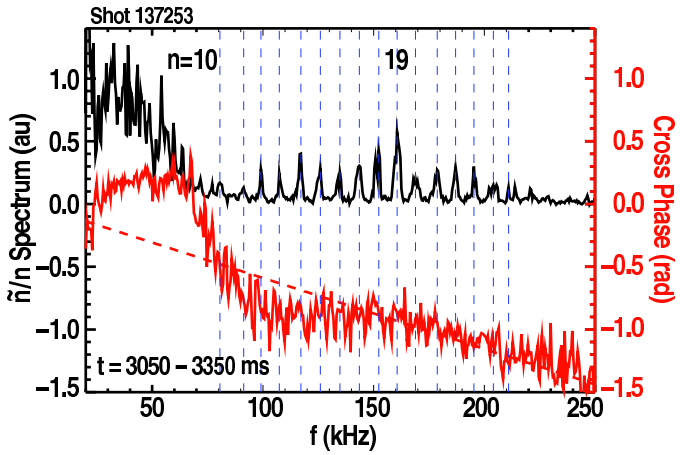

Figure 4 LX12737 28JUN2011

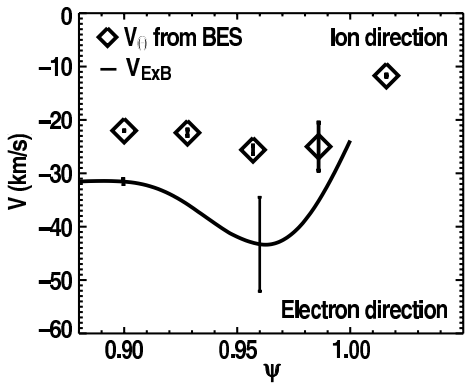

Figure 5 LX12737 28JUN2011

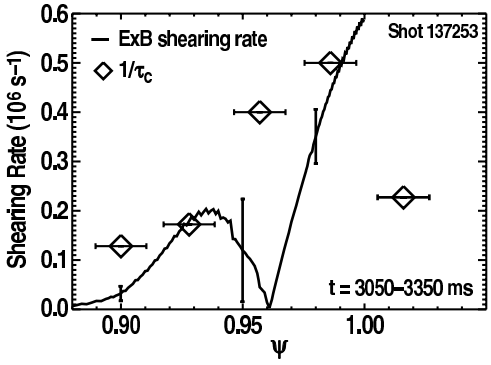

Figure 6 LX12737 28JUN2011